

# APPLICATION OF SENSORLESS SLIDING MODE OBSERVER IN CONTROL OF INDUCTION MOTOR DRIVE

*Chau Si Thien DONG<sup>1</sup>, Hau Huu VO<sup>1</sup>, Thinh Cong TRAN<sup>1</sup>,  
Pavel BRANDSTETTER<sup>2</sup>, Petr SIMONIK<sup>2</sup>*

<sup>1</sup>Department of Automation Engineering, Faculty of Electrical and Electronics Engineering, Ton Duc Thang University, 19 Nguyen Huu Tho street, Tan Phong ward, District 7, Ho Chi Minh City, Vietnam

<sup>2</sup>Department of Electronics, Faculty of Electrical Engineering and Computer Science, VSB–Technical University of Ostrava, 17. listopadu 15/2172, 708 33 Ostrava, Czech Republic

dongsithienchau@tdt.edu.vn, vohuuhaul@tdt.edu.vn, trancongthinh@tdt.edu.vn,  
pavel.brandstetter@vsb.cz, petr.simonik@vsb.cz

DOI: 10.15598/aece.v15i5.2626

**Abstract.** *Induction motors are widely used in an industry and it is necessary to improve control methods for induction motors to increase the efficiency of them. In this paper, sliding mode controllers are proposed instead of traditional PI controllers in vector control of induction motor drives. Moreover, rotor speed is estimated by a sliding mode observer. In addition, the robustness of control and observer algorithms are also proved by Lyapunov's criterion. The experiments are obtained in different speed changes of an induction motor drive. These experimental results confirm the dynamic properties of a sensorless sliding mode control of an induction motor drive.*

## Keywords

*Induction motor, Lyapunov, sliding mode control, sliding mode observer, vector control.*

## 1. Introduction

Induction motors are a type of AC electrical drives. They are widely used because they are robust, sturdy and require low maintenance. However, control of an induction motor is very difficult because of variable frequency, complex dynamic and parameter variation, etc. [1].

Vector control is one the most popular methods for controlling induction motor drives because of efficiency in a wide speed range. However, in traditional vector

control, PI controllers are used. PI controllers depend on parameters of the system and are sensitive to external noise. Sliding mode control was introduced in 1977, which overcomes disadvantages of PI control [1]. However, disadvantage of sliding mode control is chattering phenomenon. In recent years, many researchers have been involved in solving problems such as fuzzy sliding mode control [4], rotor resistance estimation [3], chattering reducing [1], etc.

During last years, sensorless control of AC machine has been developed. Sensorless means that the rotor speed is estimated from an observer or an estimator such as Extended Kalman Filter (EKF), Model Reference Adaptive System (MRAS) [5], Luenberger Observer (LO), Sliding Mode Observer (SMO) [2] and [6], etc. Sensorless control increases the reliability and decreases cost and complexity of the system. Among them, MRAS and EKF are suitable for applications with a medium speed. In contrast, LO and SMO are robust to noise and parameter variation [7].

In this paper, integral sliding mode control is proposed in controlling of induction motor drives. Moreover, a sliding mode observer is used to estimate rotor speed. Firstly, a mathematical description of the induction motor is derived. Next, the sliding mode observer, sliding mode controller and the proof of their robustness are in the second part. The structure of the sensorless sliding mode control of the induction motor is introduced in the third part. A laboratory stand is built and some experimental results are presented in the fourth part. Finally, some conclusions are summarized.

## 2. Mathematical Model of Induction Motor

The state representation of an induction motor is:

$$\begin{aligned}\dot{\mathbf{x}} &= \mathbf{A} \cdot \vec{x} + \mathbf{B} \cdot \vec{u}, \\ \mathbf{y} &= \mathbf{C} \cdot \vec{x},\end{aligned}\quad (1)$$

where  $\vec{x} = [i_{S\alpha}, i_{S\beta}, \psi_{R\alpha}, \psi_{R\beta}]^T$  is the state vector,  $\vec{u} = [u_{S\alpha}, u_{S\beta}]^T$  is the input vector and  $\vec{y}$  is the output vector.  $\mathbf{A}$ ,  $\mathbf{B}$  and  $\mathbf{C}$  are the state matrix, the input matrix and the output matrix, respectively; and

$$\mathbf{A} = \begin{bmatrix} a_{11} & a_{12} & a_{13} & a_{14} \\ a_{21} & a_{22} & a_{23} & a_{24} \\ a_{31} & a_{32} & a_{33} & a_{34} \\ a_{41} & a_{42} & a_{43} & a_{44} \end{bmatrix}, \quad (2)$$

$$\mathbf{B} = \frac{1}{\sigma \cdot L_s} \cdot \begin{bmatrix} 1 & 0 \\ 0 & 1 \\ 0 & 0 \\ 0 & 0 \end{bmatrix}, \quad (3)$$

$$\mathbf{C} = \begin{bmatrix} 1 & 0 & 0 & 0 \\ 0 & 1 & 0 & 0 \end{bmatrix}, \quad (4)$$

$$a_{11} = a_{22} = -\frac{(L_m^2 \cdot R_R + L_R^2 \cdot R_S)}{\sigma \cdot L_S \cdot L_R^2}, \quad (5)$$

$$a_{12} = a_{21} = 0, \quad (6)$$

$$a_{13} = a_{24} = \frac{L_m \cdot R_R}{\sigma \cdot L_S \cdot L_R^2}, \quad (7)$$

$$a_{14} = -a_{23} = \frac{L_m \cdot \omega_R}{\sigma \cdot L_S \cdot L_R}, \quad (8)$$

$$a_{31} = a_{42} = \frac{L_m \cdot R_R}{L_R}, \quad a_{32} = a_{41} = 0, \quad (9)$$

$$a_{33} = a_{44} = -\frac{R_R}{L_R}, \quad a_{34} = -a_{43} = -\omega_R, \quad (10)$$

where  $i_{S\alpha}$  and  $i_{S\beta}$  are stator current components,  $u_{S\alpha}$  and  $u_{S\beta}$  are stator current components,  $\psi_{R\alpha}$  and  $\psi_{R\beta}$  are rotor current components in the stator coordinate system  $[\alpha, \beta]$  respectively;  $R_S$  and  $R_R$  are stator and rotor resistances, respectively;  $L_S$  and  $L_R$  are stator and rotor inductances;  $L_m$  is the mutual inductance;  $\sigma$  is the leakage constant and  $\omega_R$  is the rotor speed.

## 3. Sensorless Sliding Mode Control of Induction Motor

In this section, a sliding mode observer and an integral sliding mode controller are developed for controlling induction motor drive.

### 3.1. Sliding Mode Observer

The sliding mode observer can be given as:

$$\begin{aligned}\dot{\hat{\mathbf{x}}} &= \hat{\mathbf{A}} \cdot \vec{\hat{x}} + \mathbf{B} \cdot \vec{u} + \mathbf{G} \cdot \text{sign}(\mathbf{S}), \\ \hat{\mathbf{y}} &= \mathbf{C} \cdot \vec{\hat{x}},\end{aligned}\quad (11)$$

where  $\hat{\mathbf{x}}$  is estimated state vector,  $\hat{\mathbf{y}}$  is the estimated output vector,  $\mathbf{G}$  is the gain matrix of the sliding mode observer,  $\mathbf{S}$  is the sliding mode surface.  $\mathbf{G}$  and  $\mathbf{S}$  are defined as:

$$\mathbf{S} = \mathbf{y} - \hat{\mathbf{y}} = \begin{bmatrix} i_{S\alpha} - \hat{i}_{S\alpha} \\ i_{S\beta} - \hat{i}_{S\beta} \end{bmatrix}, \quad (12)$$

$$\mathbf{G} = \begin{bmatrix} g_1 & -g_2 \\ g_2 & g_1 \\ g_3 & -g_4 \\ g_4 & g_3 \end{bmatrix}. \quad (13)$$

The rotor speed is estimated online by a PI controller as following:

$$\hat{\omega}_R = K_{P\omega} \cdot z_\omega + K_{I\omega} \cdot \int z_\omega dt, \quad (14)$$

where  $K_{P\omega}$ ,  $K_{I\omega}$  are proportional and integral constant of a PI controller, and  $z_\omega = (i_{S\alpha} - \hat{i}_{S\alpha}) \cdot \hat{\psi}_{R\beta} - (i_{S\beta} - \hat{i}_{S\beta}) \cdot \hat{\psi}_{R\alpha}$ .

### 3.2. Sliding Mode Control

In this section, the sliding mode control is proposed. A sliding mode controller is designed in two steps: choosing a sliding mode surface and choosing control signals.

Integral sliding mode surfaces are chosen as:

$$S_x = \int (i_m^* - i_m) dt + c_x \cdot (i_m^* - i_m), \quad (15)$$

$$S_y = \int (\omega_m^* - \omega_m) dt + c_y \cdot (\omega_m^* - \omega_m), \quad (16)$$

where  $S_x$  and  $S_y$  are sliding surfaces,  $i_m^*$  is the reference magnetizing current amplitude,  $i_m$  is the actual magnetizing current amplitude,  $\omega_m^*$  is the reference mechanical speed and  $\omega_m = (2/p) \cdot \omega_R$  is the actual mechanical speed with  $p$  is the number of poles of induction motor.

In Eq. (15) and Eq. (16), the  $c_x$  and  $c_y$  are chosen to get the desired characteristics. The flux current component and torque current component are:

$$\begin{aligned}i_{Sx}^* &= \frac{T_R}{c_x} \cdot (i_m^* - i_m) + \\ &+ i_m + \frac{T_R}{c_x} \cdot K_x \cdot \text{sign}(S_x),\end{aligned}\quad (17)$$

$$\begin{aligned}i_{Sy}^* &= \frac{J}{c_y \cdot K_T} \cdot (\omega_m^* - \omega_m) + \\ &+ \frac{J}{c_y \cdot K_T} \cdot K_y \cdot \text{sign}(S_y),\end{aligned}\quad (18)$$

where  $T_R = L_R/R_R$  is the rotor time constant,  $K_T$  is the proportional constant between the motor torque and the torque current component,  $J$  is the moment of inertia.

Suppose that the rotor time constant and the load torque are changed but are bounded as:

$$\left| \frac{\Delta T_R}{T_R} \right| \leq D_{T_R}, \quad (19)$$

$$|T_L| \leq D_{T_L}. \quad (20)$$

The system is asymptotic stable if and only if  $K_x$  and  $K_y$  satisfy:

$$K_x > D_{T_R} \cdot |i_m^* - i_m|, \quad (21)$$

$$K_y > D_{T_L} \cdot \frac{c_y}{J}. \quad (22)$$

**Proof:**

The Lyapunov function is chosen as:

$$V = \frac{1}{2} \cdot (S_x^2 + S_y^2). \quad (23)$$

The Eq. (23) is positive definite function. The first derivative of Lyapunov function is:

$$\dot{V} = S_x \cdot \dot{S}_x + S_y \cdot \dot{S}_y. \quad (24)$$

The Eq. (24) is negative definite function if:

$$\dot{S}_x = -K_x \cdot \text{sign}(S_x), \quad (25)$$

$$\dot{S}_y = -K_y \cdot \text{sign}(S_y), \quad (26)$$

where  $\text{sign}$  is the signum function:

$$\text{sign}(x) = \begin{cases} 1, & x > 0, \\ -1, & x = 0, \\ 1, & x < 0, \end{cases} \quad (27)$$

We have:

$$\dot{S}_x = (i_m^* - i_m) - c_x \cdot \frac{1}{T_R} \cdot (i_{Sx} - i_m). \quad (28)$$

Replace  $i_{Sx}$  in Eq. (17) into Eq. (28), Eq. (28) becomes:

$$\begin{aligned} \dot{S}_x &= \frac{\Delta T_R}{T_R + \Delta T_R} (i_m^* - i_m) - \\ &+ K_x \cdot \frac{1}{T_R + \Delta T_R} \cdot \text{sign}(S_x). \end{aligned} \quad (29)$$

The first derivative of  $S_x$  has the opposite sign with  $S_x$  so condition for  $K_x$  is derived as in Eq. (21). Next, the first derivative of  $S_y$  is:

$$\dot{S}_y = c_y \cdot \frac{1}{J} \cdot T_L - K_y \cdot \text{sign}(S_y). \quad (30)$$

Similarly, the first derivative of  $S_y$  has the opposite sign with  $S_y$  and the condition for  $K_y$  is in Eq. (22).

Therefore, with the control signals as in Eq. (17) and Eq. (18) and with the condition of  $K_x$  and  $K_y$  as in Eq. (21) and Eq. (22), the system is asymptotic stable. However, to eliminate the chattering problem, the saturation is used instead of signum function in Eq. (17) and Eq. (18).

## 4. Sensorless Sliding Mode Control Structure of Induction Motor Drive

The control structure of Induction Motor (IM) drive is shown as in Fig. 1. This figure is the basic scheme of vector control of an induction motor drive but PI controllers in speed control loop and flux control loop are replaced by Sliding Mode Controllers (SMC). A sliding mode observer is used to estimate rotor speed and a current model is used to estimate the rotor flux components. The control of induction motor is described step by step as follows:

- Step 1:  $i_{Sa}$ ,  $i_{Sb}$  are measured by current sensors.
- Step 2:  $i_{S\alpha}$ ,  $i_{S\beta}$  are calculated from  $i_{Sa}$ ,  $i_{Sb}$ .
- Step 3: The stator angle  $\hat{\gamma}$  and rotor flux components are estimated by a current model.
- Step 4: Calculate  $i_{Sx}$ ,  $i_{Sy}$  from  $i_{S\alpha}$ ,  $i_{S\beta}$  and  $\hat{\gamma}$ .
- Step 5: Calculate  $i_{Sx}^*$  and  $i_{Sy}^*$  by sliding mode controllers as in Eq. (17) and Eq. (18).
- Step 6: Calculate the reference stator voltage components  $u_{Sx}^*$  and  $u_{Sy}^*$  by PI controllers.
- Step 7:  $u_{S\alpha}^*$  and  $u_{S\beta}^*$  are calculated from  $u_{Sx}^*$  and  $u_{Sy}^*$  with the  $\hat{\gamma}$  from step 3.
- Step 8: Calculate  $u_{Sa}^*$ ,  $u_{Sb}^*$  and  $u_{Sc}^*$  and feed to PWM to control induction motor.
- Step 9: The  $u_{S\alpha}$ ,  $u_{S\beta}$ ,  $i_{S\alpha}$  and  $i_{S\beta}$  are input of sliding mode observer, which estimates the rotor speed. The stator voltage components  $u_{S\alpha}$  and  $u_{S\beta}$  depends on the  $u_{S\alpha}^*$  and  $u_{S\beta}^*$  and the used method of Pulse Width Modulation (PWM), sine PWM or space vector PWM.

## 5. Experimental Results

A laboratory stand with an induction motor drive is designed for the experimental verification of the chosen algorithms. The experimental platform is shown

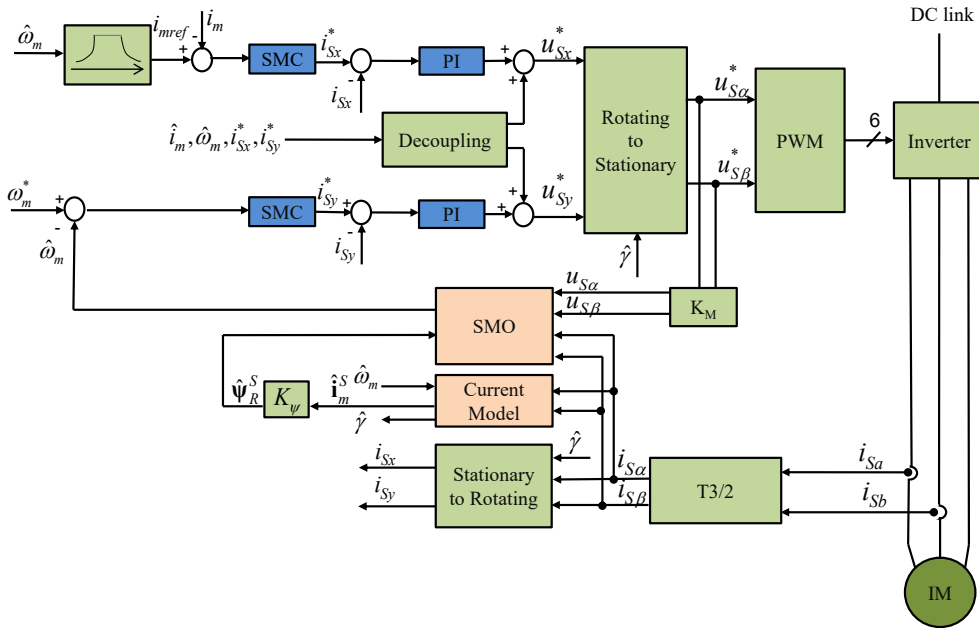


Fig. 1: Sensorless sliding mode control structure of induction motor drive.

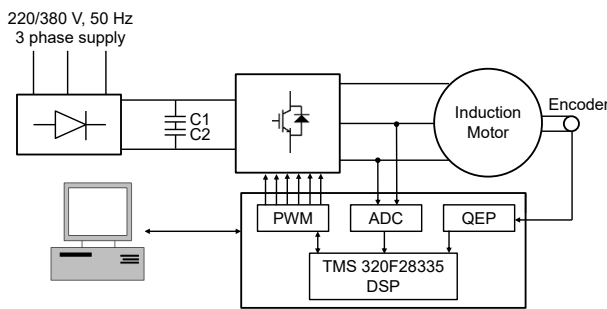


Fig. 2: Laboratory stand of control of the induction motor.

in Fig. 2. In the laboratory stand, a Siemens induction motor with the catalog number 1LA7106-4AA10 is used. Parameters of the induction motor are given in Tab. 1. At the end of the induction motor, an incremental sensor is mounted and its resolution is 3000 pulses per revolution. The induction motor is connected to an indirect frequency converter with the voltage DC-link, which was designed at the Department of Electrical Power Engineering, VSB–Technical University of Ostrava. The control of the voltage inverter is performed by the sinusoidal pulse width modulation with control frequency 10 kHz and control amplitude 10 V. Therefore, the transfer constant  $K_M$  is 1/2.

The control system is a Digital Signal Processing (DSP) of Texas Instrument eZdsp™F28335 because it is highly integrated and is a high performance solution for a demanding control application. The most important part of program is ADC interrupt subroutine, which is done for every 50  $\mu$ s. Setting reference speed, measuring current components, calculating current and flux components as well as control signals, etc.

are done in this subroutine. The load torque is from an electro-dynamometer. At the speed of 100 rpm, the maximum load torque is just 1.5 Nm.

Tab. 1: Parameters of the induction motor.

Parameter	Value
Rated power	2.2 kW
Rated speed	1420 rpm
Rated voltage	230/400 V
Rated current	8.43 A/4.85 A
Rated torque	14.8 Nm
Number of pole pairs	2
Stator resistance	3.44 $\Omega$
Stator inductance	0.1546 H
Rotor resistance	1.7178 $\Omega$
Rotor time constant	0.09 s
Moment of inertia	0.005 kg·m <sup>2</sup>

In our laboratory, the data are stored in the memory of DSP and then transferred to the MATLAB environment to draw responses. The sampling time is chosen as 10 ms. Because of the limitation of memory of the DSP, the response time is 4 s and the response of speed is divided into two cases with and without load. Without load, the reference speed is 100 rpm in the forward rotation and 60 rpm in the reverse rotation. With load, the reference speed is chosen as 100 rpm and the load torque of 1.5 Nm is added at the time of 1.5 s.

Figure 3, Fig. 4, Fig. 5, Fig. 6 and Fig. 7 show the time response of important parameters of the induction motor drive, which were obtained by measurement from the laboratory stand in case of no load. When having load, the time response of rotor speed, torque and magnetizing current component and flux current component are in Fig. 8, Fig. 9 and Fig. 10, respectively.

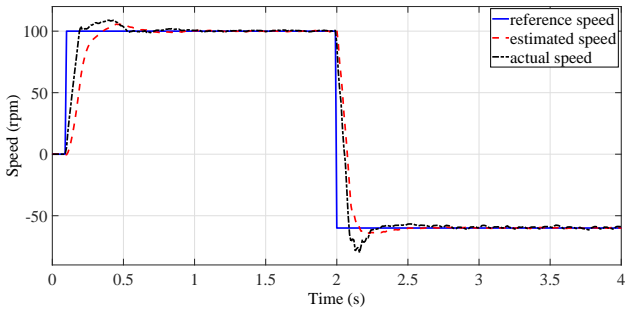


Fig. 3: Reference speed (blue), real speed (black), estimated speed (red).

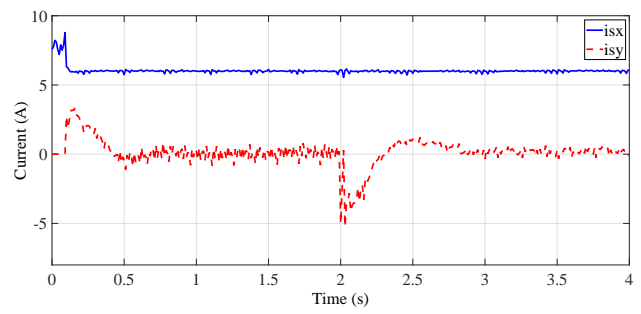


Fig. 7: Magnetizing current component and flux current component.

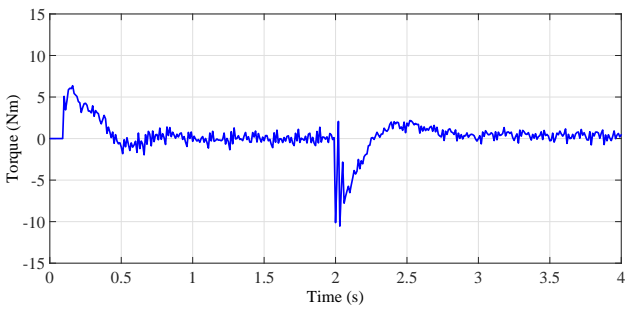


Fig. 4: Induction motor torque.

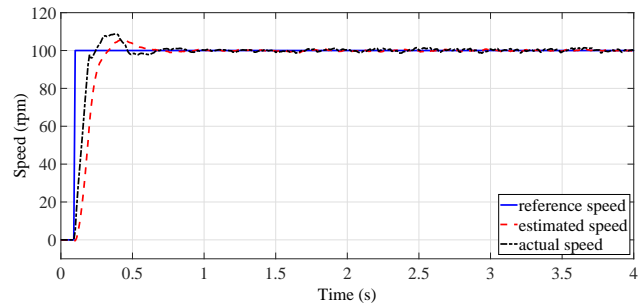


Fig. 8: Reference speed (blue), real speed (black), estimated speed (red).

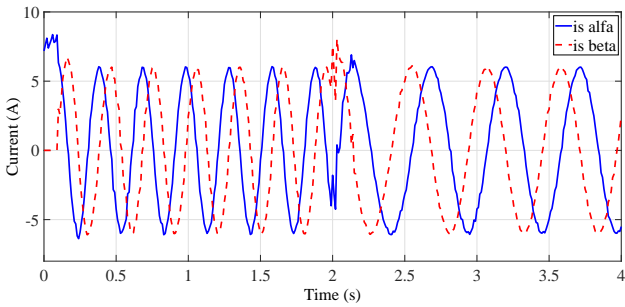


Fig. 5: Stator current vector components  $i_{S\alpha}$  and  $i_{S\beta}$ .

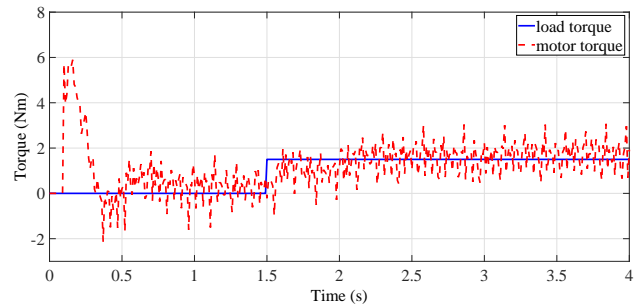


Fig. 9: Induction motor torque (red) and reference load torque (blue).

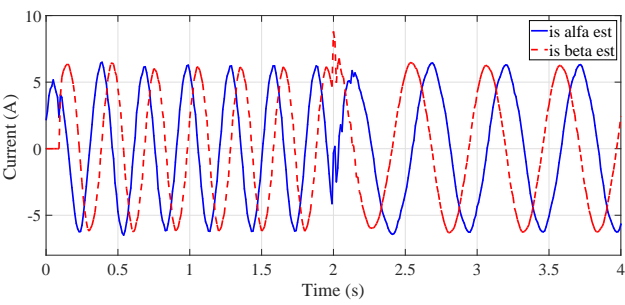


Fig. 6: Estimated stator current vector components  $\hat{i}_{S\alpha}$  and  $\hat{i}_{S\beta}$ .

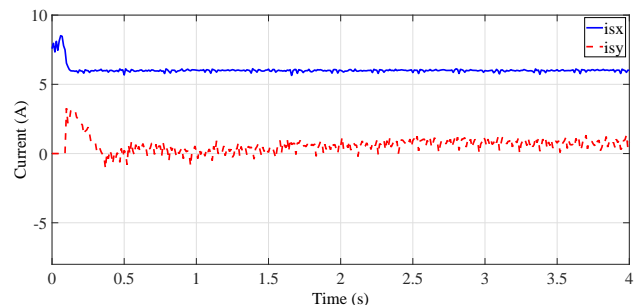


Fig. 10: Magnetizing current component and flux current component.

The response of speed is good, the percentage of overshoot is 9 %, the time response is 0.7 s and the error between the reference speed and the actual speed is just about 1 rpm. The speed decreases to 98.5 rpm at the load. After the control process, the speed re-

turns to the value corresponding to the reference speed (see Fig. 8).

## 6. Conclusion

In this paper, the sensorless sliding mode control with sliding mode observer is presented in a low speed range. The theoretical assumptions are verified through simulations in MATLAB-Simulink environment and experiments on laboratory stand. The estimated rotor speed can be used in the speed control of the induction motor drive. The absolute error between the reference speed and the actual speed in sensorless sliding mode control of the induction motor is just 1 rpm without load and 1.5 rpm with load at the reference speed of 100 rpm (percentage of error is just 1 % to 1.5 %). When comparing with PI controllers, sliding mode controllers give better results, the relative size of overshoot is smaller, settling error is smaller as well and it is more robust to external noise. When having load torque, in sliding mode control, the decreasing of rotor speed is smaller than in PI control.

## Acknowledgment

This paper was supported by the projects: Centre for Intelligent Drives and Advance Machine control (CIDAM) project, Reg. No. TE02000103 funded by the Technology Agency of the Czech Republic and Project Reg. No. SP2017/104 funded by the Student Grant Competition of VSB–Technical University of Ostrava.

## References

- [1] OLIVEIRA, C. M. R., M. L. AGUIAR, J. B. A. MONTEIRO and W. C. PEREIRA. Vector Control of Induction Motor using a Sliding Mode Controller with Chattering Reduction. In: *IEEE 13th Brazilian Power Electronics Conference and 1st Southern Power Electronics Conference (COBEP/SPEC)*. Fortaleza: IEEE, 2015, pp. 1–6. ISBN 978-1-4799-8779-5. DOI: 10.1109/COBEP.2015.7420071.
- [2] KIM, J., J. KO, J. LEE and Y. LEE. Rotor Flux and Rotor Resistance Estimation Using Extended Luenberger-Sliding Mode Observer (ELSMO) for Three Phase Induction Motor Control. *Canadian Journal of Electrical and Computer Engineering*. 2017, vol. 40, iss. 3, pp. 181–188. ISSN 0840-8688. DOI: 10.1109/CJECE.2017.2682259.
- [3] TALHAOU, H., A. MENACER and R. KECHIDA. Rotor resistance estimation using EKF for the rotor fault diagnosis in sliding mode control induction motor. In: *3rd International Conference on Systems and Control*. Algiers: IEEE, 2013, pp. 43–49. ISBN 978-1-4799-0275-0. DOI: 10.1109/ICoSC.2013.6750833.
- [4] HSU, K., H. H. CHIANG, G. H. HUANG and T. T. LEE. Enhanced fuzzy sliding mode control to motion controller of linear induction motor drives. In: *2014 IEEE International Conference on System Science and Engineering (ICSSE)*. Shanghai: IEEE, 2014, pp. 268–273. ISBN 978-1-4799-4367-8. DOI: 10.1109/ICSSE.2014.6887947.
- [5] YANG, S., X. LI, D. DING, X. ZHANG and Z. XIE. Speed sensorless control of induction motor based on sliding-mode observer and MRAS. In: *2016 IEEE 8th International Power Electronics and Motion Control Conference (IPEMC-ECCE Asia)*. Hefei: IEEE, 2016, pp. 1889–1893. ISBN 978-1-5090-1210-7. DOI: 10.1109/IPEMC.2016.7512583.
- [6] MAAMOURI, R., M. TRABELSI, M. BOUSSAK and F. M'SAHLI. Sliding mode observer sensorless vector controlled induction motor drive with anti-windup PI speed controller. In: *2016 XXII International Conference on Electrical Machines (ICEM)*. Lausanne: IEEE, 2016, pp. 1187–1193. ISBN 978-1-5090-2538-1. DOI: 10.1109/ICELMACH.2016.7732675.
- [7] ZHANG, Y., Z. ZHAO, T. LU, L. YUAN, W. XU and J. ZHU. A comparative study of Luenberger observer, sliding mode observer and extended Kalman filter for sensorless vector control of induction motor drives. In: *2009 IEEE Energy Conversion Congress and Exposition*. San Jose: IEEE, 2009, pp. 2466–2473. ISBN 978-1-4244-2893-9. DOI: 10.1109/ECCE.2009.5316508.

## About Authors

**Chau Si Thien DONG** was born in Ho Chi Minh City, Vietnam. She received her M.Sc. in Automatic Control from Ho Chi Minh City University of Technology in 2003. Her research interests include nonlinear control, adaptive control, robust control, neural network and electrical drives.

**Hau Huu VO** was born in Binh Thuan, Vietnam. He received his M.Sc. degree in Automation Engineering from Ho Chi Minh City University of Technology in 2009. His research interests include robotics, control theory and modern control methods of electrical drives.

**Thin Cong TRAN** was born in Da Nang City, Vietnam. He received his M.Sc. degree in Electrical and Electronic Engineering from Ho Chi Minh City University of Technology in 1998. His

research interests include microcontroller systems and modern control methods of electrical drives.

**Pavel BRANDSTETTER** was born in Ostrava, Czech Republic. He received his M.Sc. and Ph.D. from Brno University in 1979 and 1987, respectively. He is now full professor and dean of Faculty of Electrical Engineering and Computer Science at VSB–Technical University of Ostrava. His research interests include AC controlled drives, sensorless control and applications of observers, estimator and

soft computing methods in the control of electrical drives.

**Petr SIMONIK** was born in Ostrava, Czech Republic. He received his M.Sc. and Ph.D. from VSB–Technical University of Ostrava in 2002 and 2006, respectively. He is now vice-dean of Faculty of Electrical Engineering and Computer Science at VSB–Technical University of Ostrava. His research interests include automotive electronic systems, power active filters, and power semiconductor systems.